

# Teaching Linear Motors and Magnetic Levitation at Graduate Level

Jacek F. Gieras

**Abstract** – Linear motors and magnetic levitation have been an integral part of the graduate course “Electromechanical Energy Conversion” at the University of Technology and Life Sciences, Bydgoszcz, Poland, since 1978. The article presents small-scale laboratory prototypes of linear induction motors (LIMs), permanent magnet (PM) linear synchronous motor (LSM), electromagnetic (EML) and electrodynamic (EDL) levitation systems, which are used for teaching purposes. Introduction of linear motors and magnetic levitation to the “Electromechanical Energy Conversion” graduate course attracts more students and make this difficult course more interesting to them..

**Index Terms**—Linear motors, magnetic levitation, electromagnetic field, forces, electromechanical energy conversion, university, teaching, graduate courses.

## I. INTRODUCTION

The author would like to share his experience in teaching linear motors and magnetic levitation in the Department of Electrical Engineering at graduate level. Magnetic levitation is a part of the graduate course “Electromechanical Energy Conversion” being taught at the University of Technology and Life Sciences, Bydgoszcz, Poland since 1978. Six lecture hours out of 30 hours in total are devoted to the linear induction motors (LIM), linear synchronous motors (LSM), electromagnetic (EML) and electrodynamic (EDL) levitation and their applications in manufacturing industry, factory automation, and transportation systems. Electromechanical Energy Conversion Laboratory is equipped with a variety of small-scale prototypes of LIMs, LSMs, EML and EDL devices and systems.

## II. COURSE STRUCTURE

The course curriculum is briefly described in Table 1. The course is divided into three parts: (1) circuitual approach to analysis of electromechanical devices and systems, (2) electromagnetic field theory, 3) linear motors and magnetic levitation as examples of electromechanical components and systems. In addition to 30 lectures, 6 laboratory sessions support this course: (1) Attractive and repulsive forces of electromagnets, (2) Measurements of magnetic field distribution in the air gap of an ac. electrical machine, (3) Finite element method analysis of simple electromechanical devices, (4) Linear induction motor, (5) Linear synchronous motor, (6) EML and EDL systems (demonstration). All laboratory test benches have been built in the Electrical Engineering Department (Electrical Machines and Drives Group).

---

J. F. Gieras is with the Department of Electrical Engineering, University of Technology and Life Sciences, Bydgoszcz 85-796, Poland (e-mail: jacek.gieras@utp.edu.pl).

TABLE I  
ELECTROMECHANICAL ENERGY CONVERSION - GRADUATE COURSE AT  
UNIVERSITY OF TECHNOLOGY AND LIFE SCIENCES

Part	Topic	Lecture hours
1	Hamilton's principle	3
	Basic coordinates and parameters of systems	3
	Energies in process of conversion	3
	Electrical and mechanical balance equations in ABC, $\alpha$ - $\beta$ , and $d$ - $q$ reference frames	3
	Transformation of voltages, currents and fluxes in different reference frames	2
2	Fundamental equations of electromagnetic field	3
	Forces in electromagnetic field	2
	Electromagnetic power, Poynting vector	2
	Analysis of electromagnetic field in conductive bodies	
	Fundamentals of Finite Element Method	3
3	Linear electric motors	3
	Magnetic levitation	3

Introduction of linear motors and magnetic levitation makes the “Electromechanical Energy Conversion” course much more attractive to students than in the case of using classical electrical machines as numerical examples and laboratory equipment for experiments.

In the next sections, laboratory equipment for testing and demonstration of LIMs, LSMs, EML and EDL will be discussed.

## III. LINEAR INDUCTION MOTORS

The simplest LIM for laboratory experiments is a flat single-sided LIM with disk-type rotating secondary [6]. The laboratory set-up consists of a flat primary unit, double-layer disk with its outer diameter  $D = 0.661$  m serving as a secondary, d.c. brush machine used as a brake and instrumentation for speed and torque (force) measurements (Figs 1 and 2).

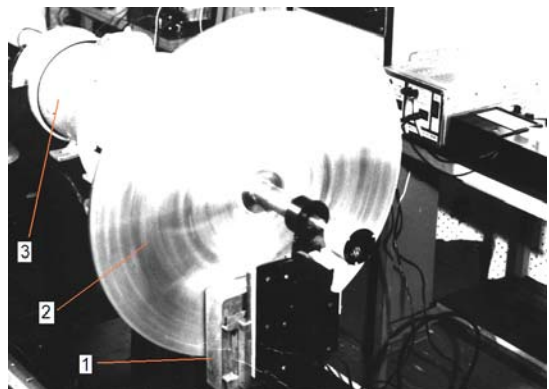


Fig. 1. Laboratory set-up with rotating disk (secondary) for testing flat single-sided LIMs. 1 – primary, 2 – secondary, 3 – d.c. machine.

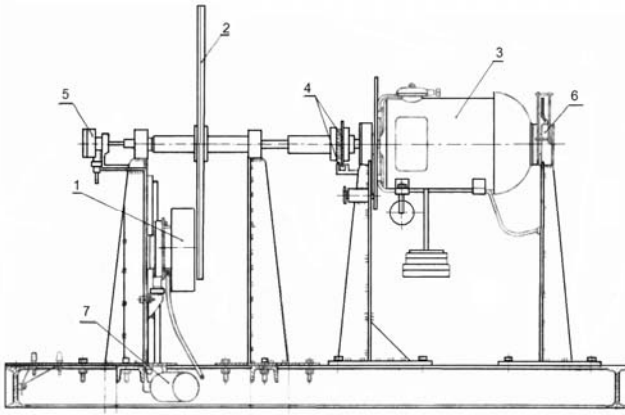


Fig. 2. Construction of laboratory set-up shown in Fig. 1. 1 – primary, 2 – disk-type secondary, 3 – d.c. machine, 4 – photoelectric tachogenerator, 5 – PM synchronous tachogenerator, 6 – torque indicator, 7 – d.c. motor for radial displacement of the primary.

The pole pitch of the primary unit is  $\tau = 50.1$  mm, number of poles  $2p = 4$ , slot pitch  $t = 16.6$  mm, effective length of the primary stack  $L = 100$  mm, number of phases  $m = 3$ , number of series connected turns per phase  $N = 490$ , diameter of bare wire  $d = 1.1$  mm, resistance per phase  $R = 3.5 \Omega$  at  $20^\circ\text{C}$ , rated line-to-line voltage  $V_L = 380$  V rms, and rated frequency  $f = 50$  Hz. The rotating disk (secondary) consists of two layers: mild steel back iron 9.5 mm thick and aluminum cap 4.7 mm thick. The ratio  $D/(2p\tau) = 3.2$ , moment of inertia of the disk  $J = 1.39$  kgm<sup>2</sup>, and the air gap between the primary and secondary (mechanical clearance)  $g = 2$  mm.

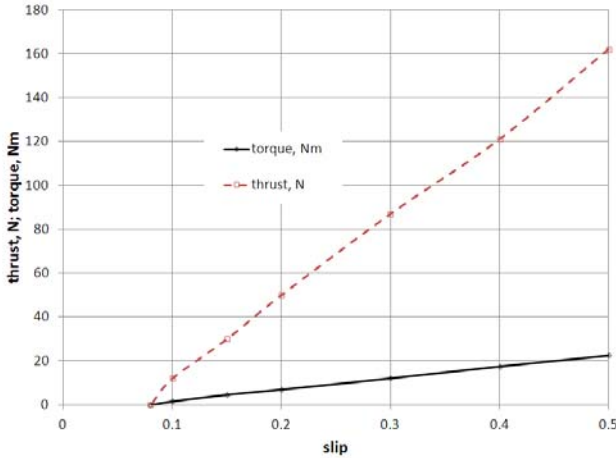


Fig. 3. Torque and thrust versus slip at  $V_L = 380$  V,  $f = 50$  Hz, and  $r = 144$  mm.

A d.c. brush machine has been used both for loading the LIM and torque measurement, because generating mode and reversible operation of the linear machine can also be investigated. In this case a 0.8 kW, 1450 rpm, 230 V d.c. separately-excited machine has been employed. The end bells of the d.c. machine have additional external bearings. The housing is equipped with a counterbalance for easy measurement of the load torque. The housing of the d.c. machine can rotate in the range of  $-90^\circ \leq \alpha \leq 90^\circ$  and is mechanically coupled with the shaft of a potentiometer. The load torque  $T_{load}$  is proportional to the sine of displacement angle  $\alpha$  of the housing of the d.c. machine, i.e.,  $T_{load} = C \sin \alpha$ , where  $C$  is a constant dependent on the mass and vertical length of the counterweight. The output voltage of the potentiometer is a linear function of the angle  $\alpha$ , i.e.,  $V_p = k \alpha$ , where  $k$  is a constant dependent on the type of potentiometer. This means, that the signal  $V_p$  must be processed further to be proportional to the load torque

$T_{load}$ . In this case, a diode electronic circuit that approximates a sine function with the aid of straight line segments has been used. Thus, the torque can be read with the aid of any analog or digital voltmeter.

To measure the rotational speed, a photoelectric tachogenerator has been used. In addition, a synchronous PM tachogenerator has also been built in (Fig. 2).

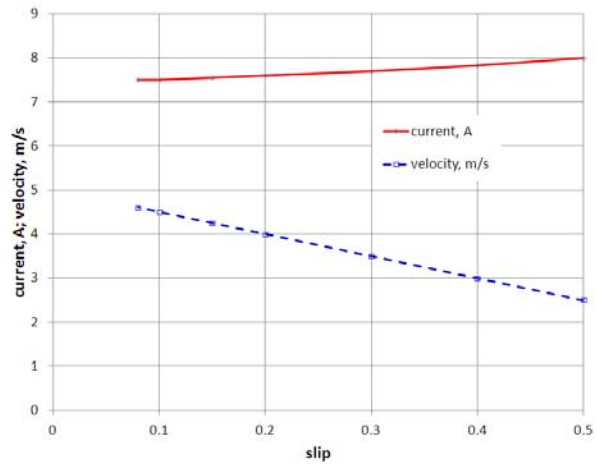


Fig. 4. Current and linear velocity versus slip at  $V_L = 380$  V,  $f = 50$  Hz, and  $r = 144$  mm.

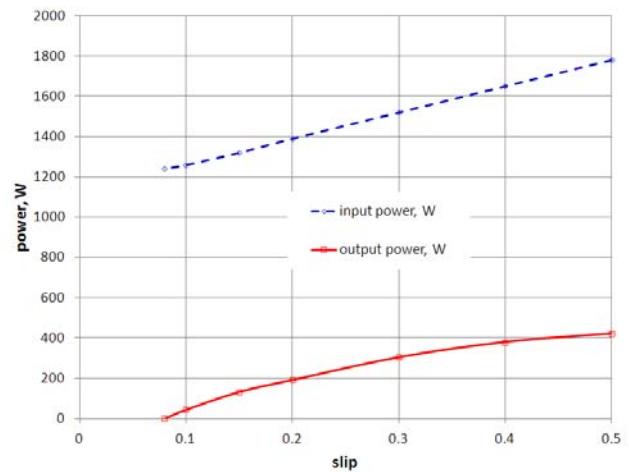


Fig. 5. Output and input active power versus slip at  $V_L = 380$  V,  $f = 50$  Hz, and  $r = 144$  mm.

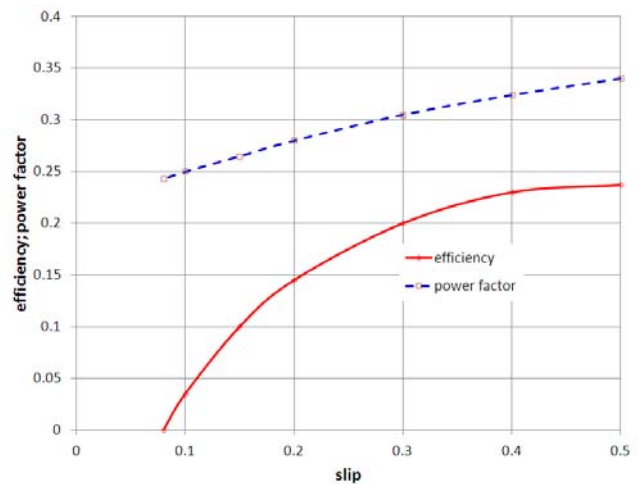


Fig. 6. Efficiency and power factor versus slip at  $V_L = 380$  V,  $f = 50$  Hz, and  $r = 144$  mm.

The primary unit of the IIM can be moved radially in the range of  $144 \leq r \leq 264$  mm with the aid of a small electric motor via step down worm gear. This additional facility is

used for the mechanical control of the speed of the rotating disk and enlarges the testing capability of the test bench.

All no-load, locked-rotor, and load characteristics for steady-state motoring mode can be easily measured. Figs. 3 to 6 show steady state load-characteristics at motoring mode measured by students. Transient characteristics at starting (acceleration) and braking (deceleration) can also be measured. When necessary, the linear machine can be tested in generating, dynamic braking (d.c. current injection), plugging, and regenerative braking modes.

The developed small-scale laboratory set up for testing flat single sided LIMs is simple, cost-effective, multifunctional, and student-resistant.

The laboratory set-up (Figs. 1 and 2) is also equipped with A-D transducers for using a PC-based data acquisition system (DAC).

To investigate a LIM-driven belt conveyor, a laboratory set-up with double-sided LIM and elastic secondary has been designed and fabricated (Figs. 7 and 8). Two primary units are the same as those used in the set-up shown in Figs 1 and 2. The belt-type secondary is designed in the form of a ladder winding with round copper bars interleaved with a woven tape, electrically and mechanically connected at each end with stranded copper wires (Fig. 8). Eddy-current brake (Fig. 7) has been used as a load.



Fig. 7. Laboratory equipment with double-sided LIM with elastic secondary for testing a small-scale LIM-driven belt conveyor.

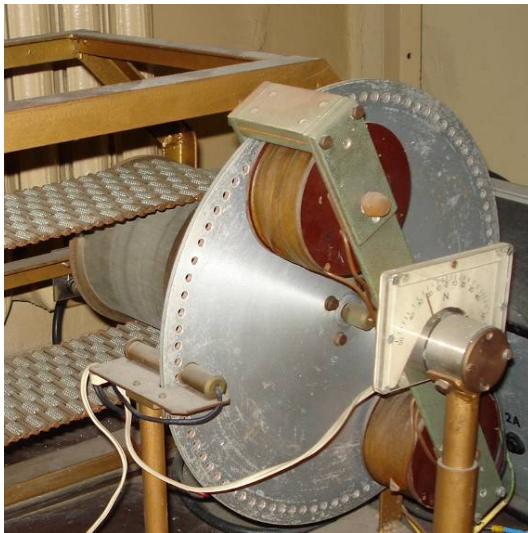


Fig. 8. Construction of belt, roller and eddy-current brake of laboratory equipment shown in Fig. 7.

This small-scale prototype of a belt conveyor with double-sided LIM is not as reliable as the set up shown in Figs 1 and 2. The main problem is the construction of a strong, thin, low electric resistance, and elastic belt that constitutes the secondary of the double-sided LIM [4]

#### IV. LINEAR SYNCHRONOUS MOTORS

A 5 m long track with PMs and short single-sided primary unit mounted on a small carriage shown in Fig. 9 constitutes a PM LSM. PM pieces are separated by mild steel poles wider than PMs to create a buried-magnet configuration of the reaction rail (Fig. 10). Buried PMs are magnetized in the direction of motion. The supporting plate corresponding to the yoke in a rotary machine is nonferromagnetic, i.e., made of aluminum. Otherwise, the bottom leakage flux between mild steel pieces would be greater than the linkage flux [8].

The carriage with three-phase primary is equipped with steel wheels, which roll on steel guide rails mounted at both sides of the track.

Since the tests on LSMs are more difficult than on LIMs, the equipment shown in Fig. 9 has only been used for demonstration. Very important is recording the speed, thrust and current profiles versus time to observe and analyze transient and steady state operation.



Fig. 9. Single sided PM LSM with moving 3-phase primary.

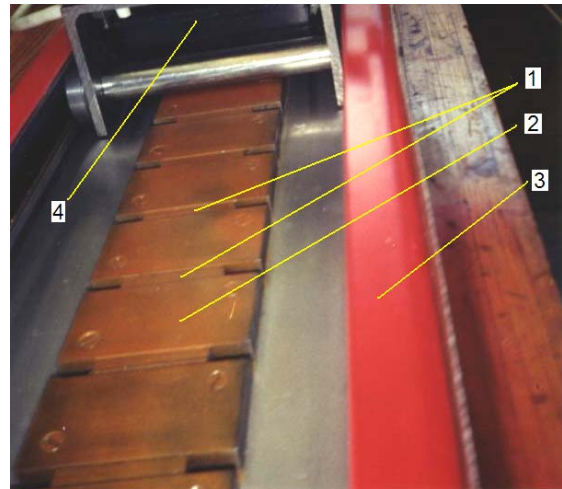


Fig. 10. Construction of stationary PM reaction rail. 1 – PM, 2 – mild steel plates, 3 – guide rail, 4 – primary.

#### V. ELECTROMAGNETIC LEVITATION

Fig. 11 shows an EML system with controlled air gap. Equation for the attraction force between U-shaped electromagnet and steel plate has been derived including the magnetic voltage drop in the ferromagnetic core (magnetic saturation) and fringing flux, i.e.,

$$F_z = \frac{\mu_0 S_g (iN)^2}{4 \left( \frac{l_{Fe}}{2\mu_r S_{Fe} / S_g} + g + z \right)^2} \quad (1)$$

where  $\mu_0 = 0.4\pi \times 10^{-6}$  H/m,  $\mu_r$  is the relative magnetic permeability of the ferromagnetic core,  $S_g$  is the cross section area of the air gap,  $S_{Fe}$  is the cross section area of

the ferromagnetic core,  $l_{Fe}$  is the length of the magnetic flux path in the ferromagnetic core and steel plate,  $g$  is the air gap,  $z$  is the vertical coordinate,  $i$  is the current and  $N$  is the number of turns.

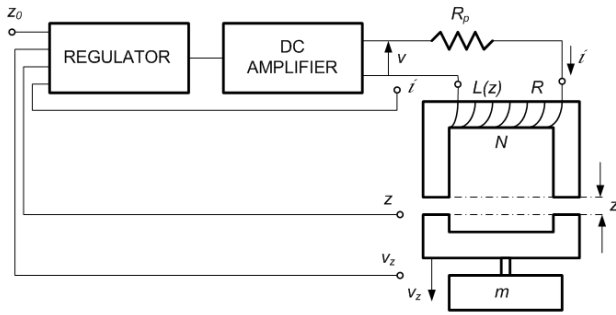


Fig. 11. EML system:  $z_0$  - required air gap,  $z$  - actual air gap,  $v_z$  - speed of the suspended mass in the  $z$ -direction,  $m$  - mass being suspended.

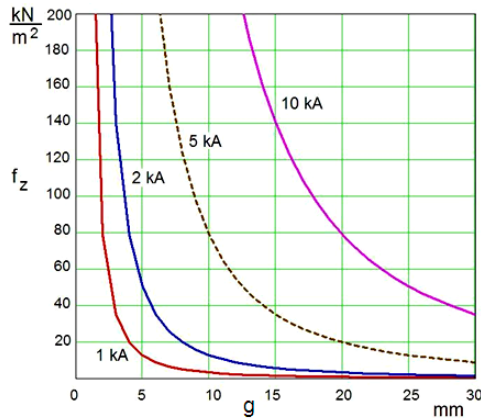


Fig. 12. Force density  $f_z$  plotted against the air gap  $g$  at constant MMF  $iN = 1, 2, 5$  and  $10$  kA.

Neglecting the magnetic saturation and assuming  $S_{Fe} \approx S_g$  the attraction force per unit area of the air gap, i.e., the force density is

$$f_z = \frac{F_z}{S_g} \approx \frac{\mu_0 (iN)^2}{4g^2} \text{ N/m}^2 \quad (2)$$

Fig. 12 shows the force density  $f_z$  plotted against the air gap  $g$  at constant MMF  $iN = \text{constant}$ .

For small fluctuations of the air gap  $g$  and current  $i$ , the force  $F_z$  can be expressed as a linear function of the air gap and current, i.e.,

$$F_z = -k_1 z + k_2 i = -m \frac{d^2 z}{dt^2} \quad (3)$$

where  $k_1, k_2$  are constants and  $m$  is the suspended mass. With zero initial conditions  $z(0) = 0, \dot{z}(0) = 0$  eqn (3) can be brought to the form

$$ms^2 Z(s) = k_1 Z(s) - k_2 i(s) \quad (4)$$

If the transfer function of the amplifier in Fig. 10 is expressed as  $i(s)/u(s) = k_3/(1+sT_m)$ , where  $u(s)$  is the control voltage signal,  $T_m$  is the amplifier time constant, and,  $k_3$  is a constant, the transfer function of the EML system is

$$\frac{Z(s)}{u(s)} = \frac{-k_2 k_3}{m(1+sT_m) \left( s^2 - \frac{k_1}{m} \right)} \quad (5)$$

Position of poles in eqn (5) shows that the system is unstable even at unlimited increase in  $k_2 k_3$  or amplification factor of the position transducer. To provide adequate reserve of stability, accuracy and fast reaction, a corrective

element (compensator) between the position transducer and power amplifier is necessary.

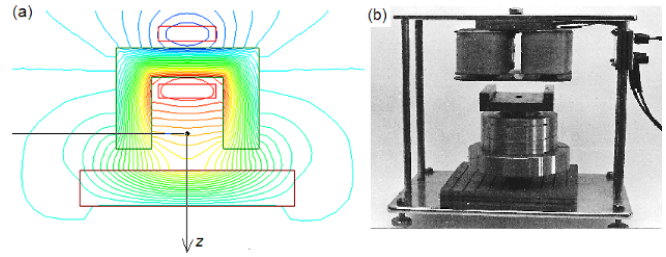


Fig. 13. Electromagnet with controlled air gap for testing EML forces: (a) magnetic flux distribution, (b) prototype.

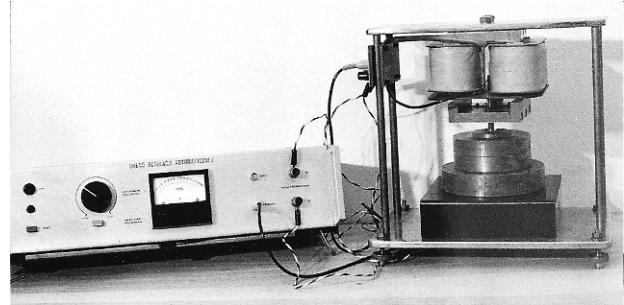


Fig. 14 Laboratory set-up for testing EML forces.

The laboratory equipment for measurements of EML forces is shown in Figs 13 and 14. This simple physical model explains the principle of operation, e.g., of German *Transrapid* maglev high speed train and Japanese HSST maglev urban transit system.

## VI. ELECTRODYNAMIC LEVITATION

A very simple and effective teaching tool for EDL is an aluminum boat-shaped object (small-scale vehicle) suspended, propelled and stabilized by the electromagnetic field excited by a long-primary transverse flux (TF) LIM. The cross section of this system and magnetic flux distribution is shown in Fig. 15.

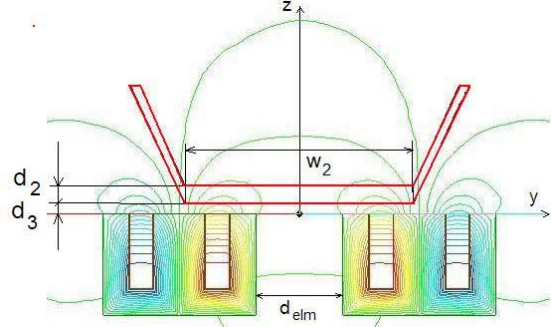


Fig. 15. Suspension of a conductive nonferromagnetic secondary in the shape of a boat with flat bottom in the magnetic field produced by a TF LIM (cross section).

If the primary winding of a flat TFLIM is fed with an a.c. current, a conductive paramagnetic or diamagnetic plate will be suspended above the primary core [1,2,3,5,9,10]. Lateral stabilization forces will be produced if the conductive plate (the secondary) is appropriately shaped [1,5,7,9,10]. It is possible to design the secondary as a "vehicle" suspended and propelled by electromagnetic field of a LIM. Figs 15 and 16 show the secondary shaped as a boat with flat bottom of a TF LIM [3,5,7,9,10].

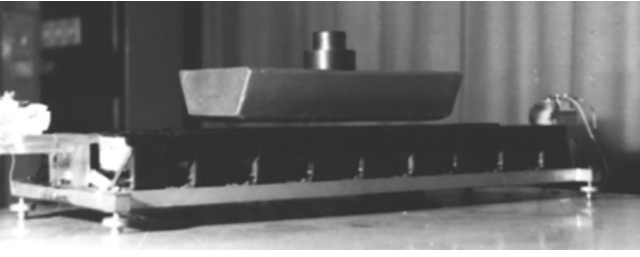


Fig. 16. Laboratory demonstration of EDL effect.

The electrodynamic force  $F_z$  in the z-direction (suspension force) can be calculated on the basis of Lorentz equation. It has been derived in [3,9].

In the most recent laboratory prototype of the TFLIM with the secondary suspended, propelled and stabilized electro-dynamically, the primary consists of 36 electromagnets with E-shape cores distributed in two rows (Fig. 17). The length of the track is 1450 mm and its width is 216 mm. The dimensions of the E-shape cores are: 56-mm height, 84-mm width, 40-mm thickness, 28-mm width of the center leg, 14-mm width of the external leg, and 14-mm height of the bottom yoke. The number of turns per electromagnet is  $N = 177$  and the diameter of round wire without insulation is 1.3 mm. The class of insulation is 220°C. The current density at 20 A *rms* is 15 A/mm<sup>2</sup>. A forced air cooling system with electric motor-driven blower has been applied. The maximum air flow can achieve 255 m<sup>3</sup>/h.



Fig. 17: The primary of the TF LIM consisting of 36 E-type electromagnets distributed in two rows and boat-shaped secondary.

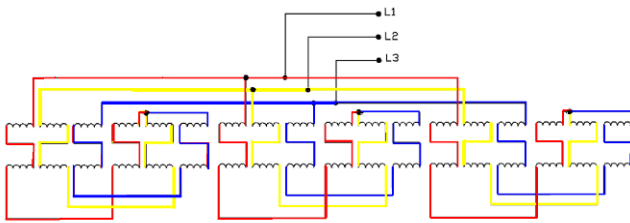


Fig. 18. Connection diagram of the primary coils to obtain unidirectional traveling magnetic field along the whole track (primary).

The connection diagram of electromagnet coils is shown in Fig. 18. Coils in Fig. 18 are connected in such a way as to obtain the traveling magnetic field along the whole length of the primary. It is also possible to connect the coils to produce only a pulsating magnetic field (single-phase excitation) or two traveling fields in opposite direction. Thus, in the second case, the secondary is kept in a stable, center position of the track (Fig. 16). Construction of the laboratory test bench with solid-state inverter and control unit is shown in Fig. 19.

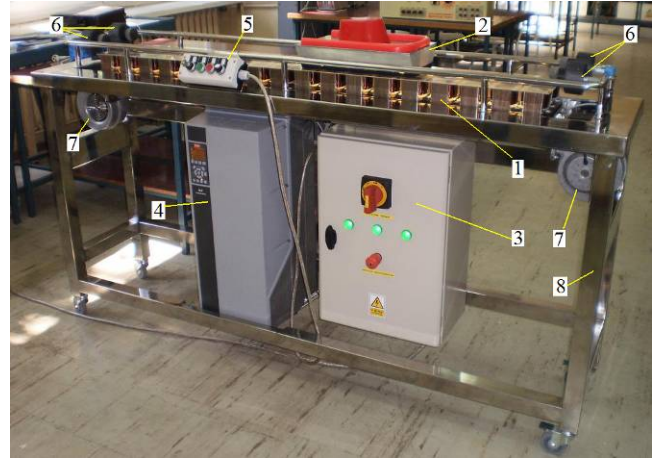


Fig. 19: Laboratory set-up for demonstration of EDL effect using a special TF LIM: 1 – primary (electromagnets), 2 – secondary, 3 – main switch and safety switch box, 4 – solid-state inverter, 5 – control unit, 6 – limit sensors, 7 – blowers, 8 – frame.

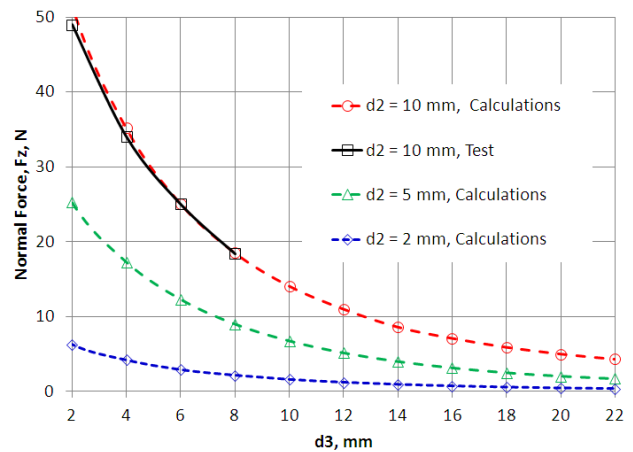


Fig. 20. Electrodynamic suspension force as a function of the air gap  $d_3$  for four different thicknesses  $d_2 = 10; 5,$  and  $2$  mm of the secondary bottom at 300 V and 50 Hz. Test results versus calculations. Calculation results on the basis of Lorentz equation [7,9].

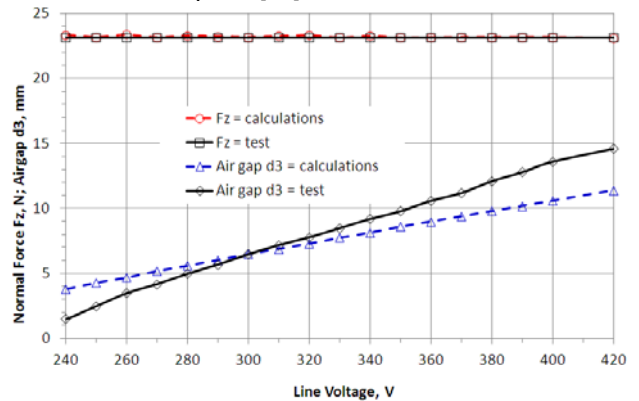


Fig. 21. Comparison of calculations of the suspension force  $F_z$  and air gap  $d_3$  with measurements at  $f = 50$  Hz and temperature of the secondary  $\theta_2 = 75^\circ\text{C}$ .

The EDL force  $F_z$  is very sensitive to the thickness  $d_2$  of the aluminum bottom of the secondary unit and the air gap  $d_3$  between the surface of electromagnets and the aluminum secondary (Fig. 20). The smaller the air gap and the thicker the secondary bottom, the higher the EDL force  $F_z$ . The electric conductivity of the secondary and its fluctuation with temperature also strongly affect the suspension force

$F_z$ . Another important effect is the so called *edge effect* that must be taken into account in calculations of the EDL force  $F_z$  [9].

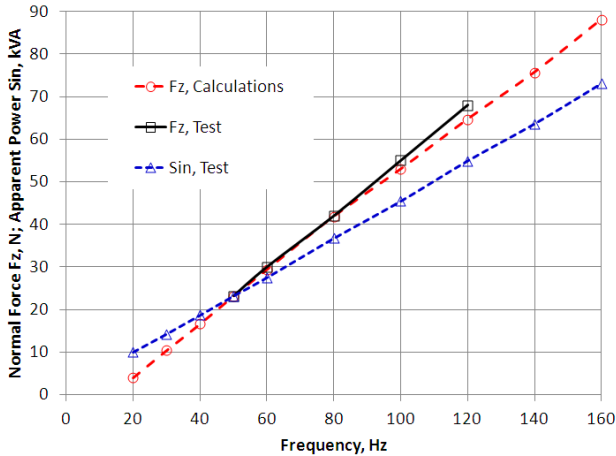


Fig. 22. Influence of the input frequency on normal force  $F_z$  and input apparent power  $S_m$  at  $d_3 = 10$  mm,  $\theta_2 = 75^\circ$  C,  $d_2 = 10$  mm,  $d_3 = 5$  mm and  $V = 300$  V. Test results versus calculations.

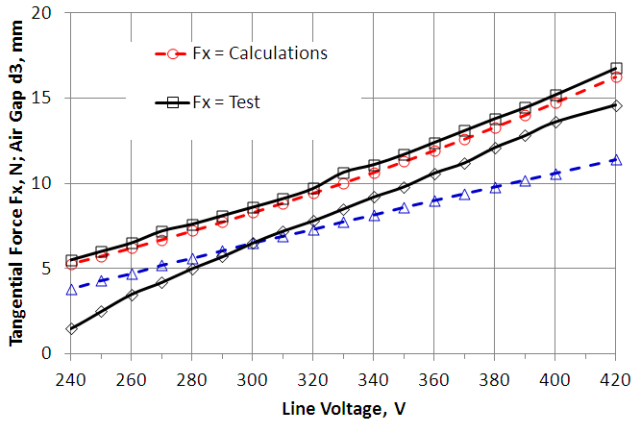


Fig. 23. Comparison of calculations of the thrust  $F_x$  with measurements at  $f = 50$  Hz and temperature of the secondary  $\theta_2 = 75^\circ$  C.

Comparison of calculation of the suspensions force  $F_z$  with test results is shown in Fig. 21.

As the input frequency increases, the suspension force  $F_z$  increases too (Fig. 22). If the frequency is doubled, the force  $F_z$  increases more than twice. Unfortunately, the input apparent power also increases with the frequency.

Tangential force  $F_x$  (thrust) produced by a TFLIM is much smaller than the suspension force  $F_z$  (Fig. 23).

The laboratory prototype of the TF LIM (Fig. 19) for the demonstration of EDL effect helps students to understand the principle of operation of the EDL maglev train on the Yamanashi Maglev Test Line (YMTL). Although, the YMTL uses superconducting electromagnets, the repulsive forces are produced in a similar way. This prototype plays also important role in public awareness of the EDL effect (University *Open Door*, science festivals, exhibitions, science education, amusement parks, etc.). Precision manufacturing industry and defense forces have shown interest in TF LIMs with the secondary suspended electro-dynamically.

## VII. OTHER SMALL-SCALE PROTOTYPES

Teaching and demonstration of linear machines and magnetic levitation is not limited to prototypes discussed in Sections III (LIM), IV (LSM), V (EML), and IV (EDL). Examples of other prototypes built as students' projects are shown in Figures 24 to 26.

In a small-scale EDL prototype shown in Fig. 24 the vehicle is suspended, propelled and stabilized with the aid of V-shaped active track and V-shaped passive bogie of the vehicle (TF LIM). A three-phase system of stationary electromagnets induces eddy current in the bottom of the vehicle. Interaction of eddy currents and magnetic field excited by the stationary track in connection with the V-shape provides all the necessary forces needed for stable operation of the system.

In Fig. 25 the small-scale vehicle is suspended by repulsive forces of PMs installed both in the track and in the vehicle and LIM. The primary of the LIM constitutes the track and the passive reaction rail of the LIM is integrated with the vehicle.

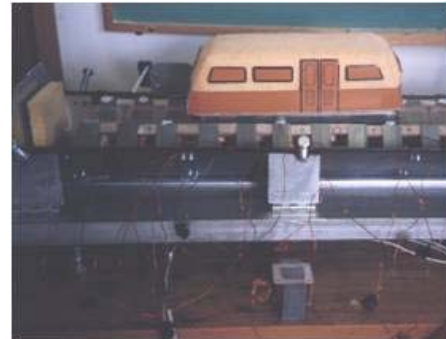


Fig. 24. Prototype of an EDL people mover suspended, propelled and stabilized using a V-shaped TF LIM



Fig. 25. Prototype of a LIM-driven people mover with permanent magnet repulsive suspension system.



Fig. 26. EML of Coca-Cola can.

Last, but not least, why is the aluminum Coca-Cola can shown in Fig. 26 suspended electromagnetically using an ELM system as that shown in Fig. 11? Aluminum is a paramagnetic material.

## VIII. CONCLUSIONS

Linear motors and magnetic levitation have been taught at the University of Technology and Life Sciences, Bydgoszcz, Poland since 1978, as a part of “Electromechanical Energy Conversion” graduate course. Six lecture hours out of 30 in total (Table 1) are devoted to LIMs, LSMs, EML and EDL, and their utilization in manufacturing industry, factory automation, and transportation systems.

A flat single-sided LIM with disk-type rotating secondary (Figs 1 and 2) is a cost-effective, easy-to-test and student resistant equipment for laboratory experiments. The laboratory set-up consists of a flat primary unit, double-layer disk with outer diameter  $D = 0.661$  m serving as a secondary, d.c. brush machine used as a brake and instrumentation for speed and torque (force) measurements.

For investigation of performance characteristics and behavior of LIM-driven belt conveyors, a laboratory set-up with double-sided LIM and elastic secondary shown in Figs. 7 and 8 has been built.

A LSM test bench has been designed and built as a 5 m track with PMs and short single-sided primary unit mounted on a small carriage (Fig. 9). To save the PM material, a buried-magnet configuration of the secondary as shown in Fig. 10 has been designed.

The EML system with controlled air gap (Figs 13 and 14) have been used to explain students the principle of operation of *Transrapid* maglev train (Shanghai, China) and HSST urban transit system (Japan).

A very simple and effective teaching tool for EDL is an aluminum boat-shaped object (small-scale vehicle) suspended, propelled and stabilized by the electromagnetic field excited by a long-primary TF LIM (Figs 16, 17, and 19). The TF LIM for the demonstration of EDL effect helps students to understand the principle of operation of high speed maglev trains on the YMTL (Yamanashi Prefecture near Tokyo, Japan).

At present time, all laboratory equipment (Figs. 1, 6, 8, 14, and 26) use PC-based DACs to measure and monitor linear motors and magnetic levitation systems under steady-state and transient operation.

Introduction of linear motors and magnetic levitation to “Electromechanical Energy Conversion” course has made this course more attractive to graduate students. Problems regarded as difficult and sometimes boring, e.g., Hamilton’s principle, Euler-Lagrange equation, Maxwell equations, etc., can become interesting to young people, if illustrated with state-of-the art power engineering technologies.

Small-scale prototypes (Figs 1, 2, 7, 8, 9, 13, 14, 16, 17, and 19), well-designed attractive power point presentations, and video movies are very important in the teaching

process. In students’ opinion (course evaluation sheets), magnetic levitation was the highest value and most interesting topic in the “Electromagnetic Energy Conversion” course.

## IX. REFERENCES

- [1] J.F. Eastham and E.R. Laithwaite, “Linear induction motors as electromagnetic rivers,” *Proc. IEE*, vol. 121, pp. 1099-1108, No 10, 1974.
- [2] E. M. Freeman, D.A. Lowther, “Normal force in single-sided linear induction motors,” *Proc. IEE*, vol. 120, pp. 1499-1506, No 12, 1973.
- [3] J.F. Gieras, “Electrodynamic forces in electromagnetic levitation systems,” *Acta Technica CSAV*, pp. 532-545, No 5, 1982.
- [4] J.F. Gieras, “Simplified theory of double-sided induction motor with squirrel-cage elastic secondary,” *IEE Proc. Pt B: Electric Power Applications*, vol. 30, , pp. 424-430, No. 6, 1983.
- [5] J.F. Gieras, “Influence of structure and material of secondary suspended electro-dynamically on steady performance characteristics of linear induction motor with transverse flux.”, *etzArchiv*, vol. 6, pp. 255-260, No 7, 1984.
- [6] J.F. Gieras, “Laboratory set-up for testing flat single-sided linear induction machines,” *Przegląd Elektrotechniczny (Electrical Review)*, Poland, vol. 60, pp. 84-89, No 3, 1984.
- [7] J. F. Gieras, *Linear induction drives*. Oxford University Press, Oxford, 1994.
- [8] J.F. Gieras, Z.J. Piech and B.Z. Tomczuk, *Linear synchronous motors*, 2<sup>nd</sup> ed. , Taylor & Francis – CRC Press, Boca Raton, 2012.
- [9] F. Gieras, J. Mews and M. Splawski, “Analytical calculation of electrodynamic levitation forces in a special-purpose linear induction motor,” *IEEE Trans on Industry Applications*, vol. 48, , pp. 106-116. No 1, 2012.
- [10] P. Hochhausler, “Der Katamaran als magnetisches Schwebefahrzeug.” *ETZ B*, vol 26, pp. 412-413, No 3, 1973.

## X. BIOGRAPHY

**Jacek F. Gieras** (M’83–SM’87–F’02) graduated in 1971 from the Technical University of Lodz, Poland, with distinction. He received his PhD degree in Electrical Engineering (Electrical Machines) in 1975 and Dr habil. degree (corresponding to DSc), also in Electrical Engineering, in 1980 from the University of Technology, Poznan, Poland. His research area is Electrical Machines, Drives, Electromagnetics, Power Systems, and Railway Engineering. From 1971 to 1998 he pursued his academic career at several Universities worldwide including Poland (Technical University of Poznan and University of Technology and Life Sciences, Bydgoszcz), Canada (Queen’s University, Kingston, Ontario), Jordan (Jordan University of Sciences and Technology, Irbid) and South Africa (University of Cape Town). He was also a Central Japan Railway Company Visiting Professor at the University of Tokyo (Endowed Chair in Transportation Systems Engineering), Guest Professor at Chungbuk National University, Cheongju, South Korea, and Guest Professor at University of Rome *La Sapienza*, Italy. In 1987 he was promoted to the rank of Professor (life title given by the President of the Republic of Poland). He is a Full Professor of Electrical Engineering at the University of Technology and Life Sciences in Bydgoszcz, Poland.

He authored and co-authored 11 books, over 250 scientific and technical papers and holds over 60 US patents and patent publications. The most important books are *Linear Induction Motors*, Oxford University Press, 1994, U.K., *Permanent Magnet Motors Technology: Design and Applications*, Marcel Dekker Inc., New York, 1996, 2nd edition 2002, 3rd edition 2010 (Taylor & Francis), *Linear Synchronous Motors: Transportation and Automation Systems*, CRC Press LLC, Boca Raton, Florida, 1999, 2<sup>nd</sup> edition 2012, *Axial Flux Permanent Magnet Brushless Machines*, Springer-Kluwer Academic Publishers, Boston-Dordrecht-London, 2004, 2nd edition 2008, *Noise of Polyphase Electric Motors*, CRC Press - Taylor & Francis, 2005, and *Advancements in Electric Machines*, Springer, Dordrecht-London-New York, 2008.